Nature's Frontiers

Achieving Sustainability, Efficiency, and Prosperity with Natural Capital

Appendix B: Technical Appendix

Richard Damania, Stephen Polasky, Mary Ruckelshaus, Jason Russ, Markus Amann, Rebecca Chaplin-Kramer, James Gerber, Peter Hawthorne, Martin Philipp Heger, Saleh Mamun, Giovanni Ruta, Rafael Schmitt, Jeffrey Smith, Adrian Vogl, Fabian Wagner, and Esha Zaveri

This document contains the technical appendix from *Nature's Frontiers: Achieving Sustainability, Efficiency, and Prosperity with Natural Capital,* doi: 10.1596/978-1-4648-1923-0. A PDF of the full book is available at https://openknowledge.worldbank.org/ and http://documents.worldbank.org/, and print copies can be ordered at www.amazon.com. Please use the full version of the book for citation, reproduction, and adaptation purposes.

B. Methods

The core approach used in the landscape portion of the report *Nature's Frontiers: Achieving Sustainability, Efficiency, and Prosperity with Natural Capital* models how spatial patterns in land use and land management (LU-LM) affect natural capital and the resulting ecosystem processes that determine the status of biodiversity and the flow of benefits to people (so-called ecosystem services). The component models used in this analysis quantify relationships between land use and land management patterns, biophysical processes, and a number of important environmental and economic benefits (see Chaplin-Kramer et al. 2019; Kareiva et al. 2011; Nelson et al. 2009; Sharp et al. 2020; references in table B.1). These component models utilize a wide array of globally available biophysical and socioeconomic data. Both the methods and the data are described in detail in this appendix.

Six important ecosystem service and biodiversity outcome categories are modeled: (1) net greenhouse gas (GHG) storage and emissions reductions, which include changes in carbon storage due to land use change as well as methane emissions from livestock production, both expressed as metric tons of carbon dioxide equivalent (CO_2eq); (2) biodiversity, which includes information on potential species richness, threatened and endangered species, endemic species, rare ecoregions, forest intactness, and key biodiversity areas; (3) water quality, measured by nitrate concentrations in drinking water supplies; (4) net returns from agricultural crop production; (5) net returns from livestock grazing; and (6) net returns from timber production. Categories 1–3 are measured in their own terms (metric tons of CO_2eq, a biodiversity metric score, and nitrate concentrations), whereas categories 4–6 are combined into a single monetary metric.

Thirteen alternative future land use and land management alternatives are modeled: natural habitat, forestry, grazing, and 10 alternatives for agricultural crop production that incorporate different management options for growing crops. Two LU-LM alternatives for agricultural crop management use current production methods—one assuming current crop area and one assuming expanded crop production area. Eight LU-LM alternatives for agricultural crop management use intensified production methods. These eight LU-LM alternatives involve all possible combinations of current production area versus expanded production area, irrigated versus rainfed, and adoption of best management practices (BMPs) versus nonadoption of BMPs.

The component models and LU-LM alternatives are incorporated into an optimization approach to arrive at a set of Pareto-efficient solutions (Polasky et al. 2008). In a Pareto-efficient solution, it is not possible to change the LU-LM alternative on any set of parcels in a country to increase the score for any one component without also reducing the score for some other component. The optimization algorithm chooses one of the 13 LU-LM alternatives for each land parcel within a country so that the resulting land use and land management pattern is Pareto optimal. The optimization analysis included five of the six benefits but excluded water quality because the water quality analysis was still in an experimental stage when the optimization analysis was being conducted.

The methods, data inputs, and key references for each of the six benefits are summarized in table B.1 and described in detail in the sections that follow. Figure B.1 illustrates the steps in going from land use and land management patterns to total net revenue from production from landscapes. Separate models for agriculture, forestry and grazing generate net revenue estimates, which are then tallied for a total

production net value as an input to the optimization modeling. Scenario descriptions, a summary of methods for each model, and the optimization approach are provided in this appendix.

Table B.1 Summary of methodology and data sources used for components of the landscape efficiency score

Component	Measure	Summary of methodology	Key data sources
Total net return from agricultural crop production, forestry, and grazing	Monetary returns from the landscape under each land use and land management (LU-LM) alternative	Net revenue from agricultural crop, forestry, and grazing production are summed for each parcel and scenario as inputs to the optimization analysis that generates the landscape efficiency score.	See below.
Agricultural crop production	Net revenue from 10 major global crops (barley, cassava, maize, oil palm, rapeseed, rice, sorghum, soybean, sugarcane, wheat) for each parcel for each agricultural crop LU-LM alternative	Potential crop yields under each scenario modeled as a function of crop-specific temperature, precipitation, soil type, etc. and whether each parcel is rainfed or irrigated and is intensively managed. Suitability of different crops per parcel, which depends on slope, weather, soil type, and sustainability of irrigation. Net revenue from crop production for each crop and parcel are equal to yield × producer price – production costs and transport costs.	FAO (2020); Mueller et al. (2012); Ray et al. (2019); Weiss et al. (2018); World Bank (2020); Zabel, Putzenlechner, and Mauser (2014)
Forestry	Net revenue from managed forestry for each parcel for the forestry LU-LM alternative	Potential forest biomass and yields are modeled as a function of vegetation types and observed growth functions. Net monetary returns from managed forestry are calculated based on regional log prices minus harvesting and transportation costs.	Favero, Daigneault, and Sohngen (2020); Kim et al. (2017); Tian et al. (2016)
Livestock production from grazing	Net revenue from livestock production expressed in terms of beef equivalents based on grass/forage	Average annual grazed biomass availability and resulting (sustainable) grazing intensity modeled	Castonguay et al. (2022); Chang et al. (2016); FAO (2021b); Herrero et al. (2013)

Component	Measure	Summary of methodology	Key data sources
	intake only (no feedlots) for each parcel for the grazing LU-LM alternative	for each parcel as beef-equivalent meat produced (kilograms per hectare) and greenhouse gas (GHG) emissions (as carbon and methane from manure and transport). Net revenue is a function of meat production × price of meat – production costs and transport costs	
Nonmonetary environmental benefits	Combined index of GHG storage and emissions reductions and the biodiversity index for each parcel for each LU-LM alternative	Geometric mean of GHG emissions and biodiversity index for each parcel/scenario	See below.
Greenhouse gas emissions	Net carbon storage minus methane emissions from livestock expressed as carbon dioxide equivalent in metric tons for each parcel for each LU-LM alternative	Above-ground and below-ground carbon pools from data for forest, herbaceous (grass and shrub) and agricultural, forest, grazing, and urban land cover classes for each of 124 global carbon zones. Methane emissions (over 20 years) were subtracted from the carbon stock for the land use/land cover (LU/LC) on a particular pixel if grazing is allowed on that pixel. GHG emissions for different LU/LC adjusted for each scenario as information allows.	Ruesch and Gibbs (2008); Suh et al. (2020)
Biodiversity	Biodiversity index comprised of six biodiversity metrics: (1) species richness, (2) habitat for species at risk; (3) habitat for endemic species; (4) habitat in rare ecoregions; (5) forest intactness; and (6) key biodiversity areas (KBAs),	Metrics: (1) species richness as a function of LU/LC from PREDICTS database, International Union for Conservation of Nature (IUCN) range maps, and European Space Agency (ESA) LU/LC; (2) amount of "natural" habitat available to species with smaller	ESA (2019); Dinerstein et al. (2017); Grantham et al. (2020); IUCN (2019); PREDICTS database (Hudson et al. [2014]; Newbold et al. [2015])

Component	Measure	Summary of methodology	Key data sources
	expressed as maximum of the indexes for each parcel for each LU-LM alternative.	ranges; (3) amount of ”natural” habitat available to species at risk from IUCN Red List; (4) overlaid map of KBAs with study’s map of natural habitat (5) calculation of inverse of each ecoregion's size to identify rare ecoregions and the amount of ”natural” habitat in each; (6) global data on forest intactness. Each metric was normalized between 0 and 1 (except KBAs, which were normalized between 0 and 0.5). The maximum of the six values is the final value for each parcel.	
Water quality–human health	Nitrate concentrations in drinking water	Nitrogen export based on fertilizer application rate, runoff (from precipitation), topography, and vegetation retention capacity located along flow path between pollutant source and stream. Nitrogen export converted to nitrate concentrations in ground and surface water using a random forest model predicting the global observed nitrate concentration based on modeled export and other covariates (basin size, climate, etc.) converted to concentrations of nitrate in drinking water based on country level statistics of drinking water sources.	Chaplin-Kramer et al. (2019); Damania et al. (2019); Gu et al. (2013); Ouedraogo, Defourny, and Vanclooster (2019)

Source: Original table for this publication.

Figure B.1 Steps to estimating total production value

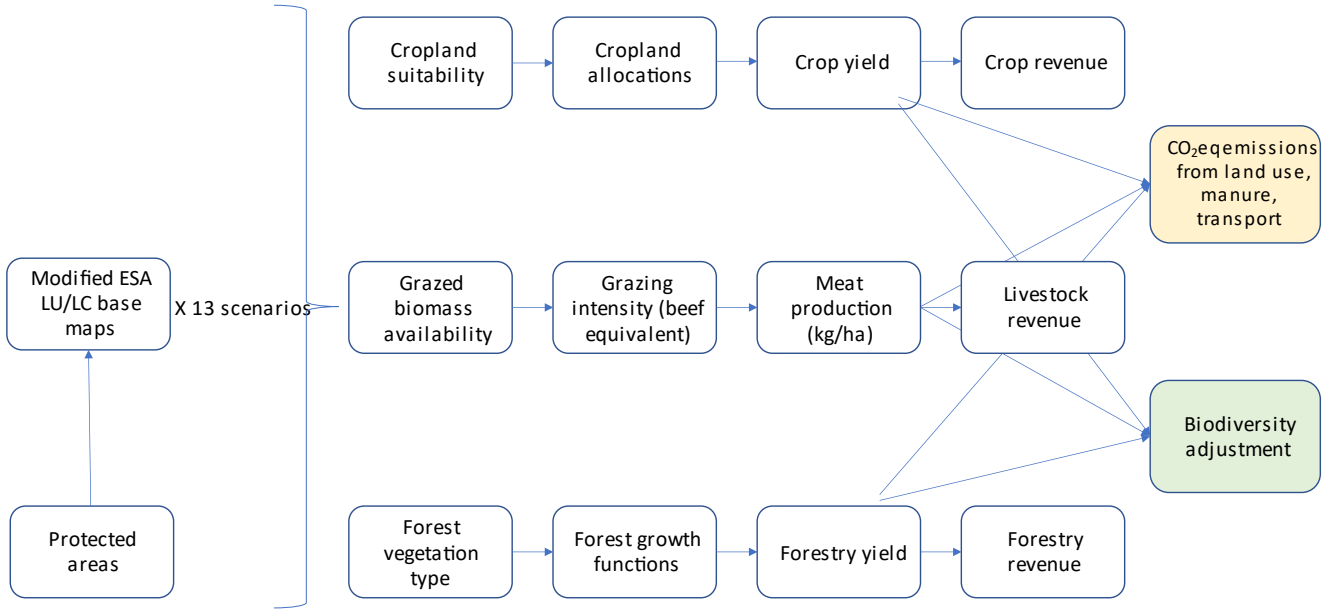

Source: Original figure for this publication.
Note: Flow diagram includes the net production for agricultural crops, grazing, and forestry for each parcel for each land use and land management alternative and the impact on nonmarket environmental components. The location and condition of ecosystems are entered in the land use/land cover (LU/LC) base maps (with over 30 distinct habitat classifications). For protected areas, only the natural land use alternative is allowed. These input maps then contribute to designated cropland suitability, grazed biomass availability, and forest vegetation type. Each ecosystem service model (crop yield, meat production, and forestry yield) uses additional ecosystem attributes to estimate service provision (such as soil type, water availability, temperature, and slope). Details on ecosystem attributes included in each model can be found in this technical appendix. ESA = European Space Agency; CO_2eq = carbon dioxide equivalent; kg/ha = kilograms per hectare.

B.1 Biodiversity and ecosystem services modeling

B.1.1 Carbon storage and reduced greenhouse gas emissions

Ecosystems regulate the earth's climate, in part by adding and removing greenhouse gases such as carbon dioxide (CO_2) from the atmosphere. The amount of carbon stored in soil and vegetation far exceeds the amount of carbon in the atmosphere (Lal 2002). By storing this carbon in soil, wood, and other biomass, ecosystems prevent CO_2 from entering the atmosphere where it would otherwise contribute to climate change. Disturbing these systems through changes in land use or land management can release large amounts of CO_2 into the atmosphere, whereas reforestation or other forms of restoration can lead to the increased storage of large amounts of CO_2 (Griscom et al. 2017). The Intergovernmental Panel on Climate Change (IPCC) estimates that 23 percent of global anthropogenic

emissions are from agriculture, forestry, and other land uses (IPCC 2021). Therefore, the ways in which humans manage terrestrial ecosystems are critical to regulating the earth's climate.

The InVEST Carbon Storage and Sequestration model (Sharp et al. 2020) scores each land use and land management alternative for the amount of carbon stored in different carbon pools (such as vegetation, soil, or litter). This study includes the cumulative amount found in above-ground and below-ground biomass (see figure B.2). It does not account for carbon in soil, leaf litter, or wood products. The amount of carbon stored in forest, herbaceous vegetation (grass and shrub), and agricultural land cover classes is taken from Ruesch and Gibbs (2008) and is geographically differentiated based on 124 different carbon zones, which, in turn, are based on bioclimatic variables and biomes (Suh et al. 2020). Thus the same land use/land cover classes contain different carbon densities in different parts of the world. To represent changes in carbon storage from the adoption of best management practices in agricultural crop production, a weighted average is taken for the value in that carbon zone for the dominant natural vegetation type (proportional to 10 percent of the area) and agricultural crop production (proportional to 90 percent of the area). Agricultural crop intensification is not assumed to change carbon storage. Although poorly managed agriculture may result in degraded soils that store very little carbon, intensification per se does not necessarily mean poor management, and this study team has no global information on soil tillage or other management practices that fundamentally affect carbon storage in agriculture. Therefore, estimating trade-offs of intensification with carbon storage were not attempted in this study.

For land managed as forestry, the study team reduced the carbon stored in forest classes by half to reflect the fact that timber is periodically harvested, which reduces above-ground carbon that grows back slowly while trees mature. For grazing lands, it did not attribute a change in carbon to the land use. Again, although it is unlikely that grazing has no effect on carbon, there is evidence in both directions: well-managed grazing can increase carbon storage, especially in soils, whereas poorly managed grazing can reduce it. Therefore, no attempt is made to represent trade-offs of moving from natural (ungrazed) grassland to grazing. However, if applying grazing causes a change in land cover (for example, from forest to grazed grassland), the change in that land cover is specified according to Ruesch and Gibbs, as specified earlier.

As for deserts, the carbon storage assigned to the natural sparse vegetation class was sometimes lower than the carbon storage assigned to potential cropland agriculture because of a lack of spatial heterogeneity in the cropland carbon storage data (that is, overestimating carbon potential in these areas). This heterogeneity led to the unintended outcome of very poor cropland being selected in the optimization to provide a carbon benefit. To address this outcome, when assigning the estimated carbon storage for cropland use, the study team set a maximum value equal to the carbon storage of the potential natural habitat type, thereby preventing the problematic case, but it has no effect in nondesert areas.

Methane emissions per year were derived from the livestock model for grazed parcels in terms of CO_2eq and were converted from kilograms (units in the livestock model) to metric tons (units in the carbon stocks data set) by multiplying by 0.001. Methane emissions per year were converted to a long-term measure to compare with carbon stocks. The per year emissions were multiplied by 20 years to calculate

a long-term methane emissions contribution. Carbon stocks were also converted to CO_2eq (multiplying carbon density by 44/12). The long-term methane emissions from livestock were then subtracted from the carbon stock to calculate an overall greenhouse gas storage and emissions reduction number. These calculations should not be considered net emissions because the land use–based carbon stocks are not sequestration; they are just avoided losses.

B.1.2 Biodiversity

Biodiversity is a crucial characteristic of nature. If nature is a basket of human lives and economies, then biodiversity is the quality of the material and the tightness of the weave of the basket. Biodiversity, defined in terms of the total variety of life on earth, encompasses all forms of life from genes to ecosystems and exhibits variability at spatial scales ranging from a soil aggregate to the globe and timescales ranging from minutes to millennia. In an attempt to tackle the enormous challenge of describing the variety of life on earth, scientists have created a plethora of methods and metrics in pursuit of quantifying current patterns of biodiversity and projecting future threats to it.

The very breadth of the research trajectories that have strengthened biodiversity science has made synthesis challenging. This challenge has become increasingly apparent with both the unprecedented proliferation in globally available biodiversity metrics and the call for international agreement on how to best measure biodiversity in support of the post-2020 goals of the Convention on Biological Diversity (CBD). It is unlikely a single metric will be selected by the CBD for the post-2020 goals, but rather some aggregate metric that pulls from the many groups doing great work in this space.

For the landscape efficiency score approach to biodiversity, six types of biodiversity data are combined: species richness, habitat for endemic species, habitat for threatened and endangered species, Key Biodiversity Areas, habitat for rare species, and forest intactness (figure B.2). These types account for different levels of biological organization (species and ecosystems) as well as the level of threat to that component of biodiversity (such as endangered species and range-restricted species).

Figure B.2 Conceptual model of methods used to develop the biodiversity index

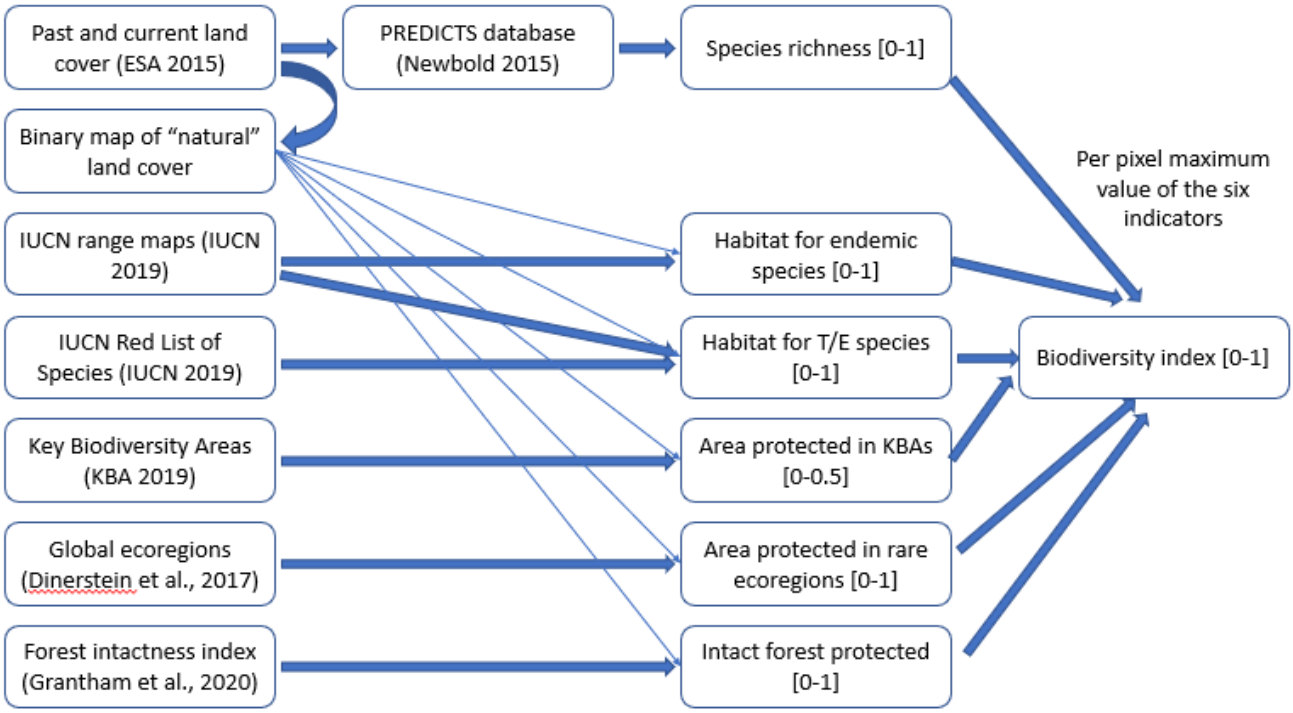

Source: Original figure for this publication.
Note: [0-1] and [0-0.5] indicate the range of potential scores that each component can receive, before being aggregated into the full Biodiversity index. IUCN = International Union for Conservation of Nature; KBA = Key Biodiversity Area; T/E = threatened and endangered.

Species richness. Species richness is the number of species represented in an ecological community, landscape, or region. It remains by a wide margin the most identifiable and relatable component of biodiversity for policymakers and decision makers. The study team used the PREDICTS database (Hudson et al. 2014; Newbold et al. 2015) to address how changes in land use and land cover affect species richness. This database is a global effort to collate primary studies in which researchers have compared the species richness and abundance associated with different types of land use and among different levels of land use intensity. A complete description of the taxonomic, geographic, and land use coverage can be found in Hudson et al. (2014).

The study team first calculated regional species pools for every land pixel in every country using IUCN range maps for amphibians, birds, mammals, and reptiles (IUCN 2019). It then modified regional species pools by the local land cover in each pixel based on European Space Agency (ESA) land cover data (ESA 2019) and the PREDICTS database. Three factors were considered:

1. General land use type (natural, plantation forest, cropland, pasture, urban area)
2. Level of human intensity (minimal, light, heavy)
3. Age of habitat for natural habitat type (young, intermediate, mature, primary).

This approach provides for each scenario a value of total species richness for every taxon in every location on the landscape. These were weighted by first dividing by the total number of species globally for each species group and then summing over all four taxa.

Habitat for endemic species. Endemic species exist in only one region, potentially increasing their risk of extinction. The amount of habitat available for endemic species was mapped using European Space Agency land use/land cover data (ESA 2015). Degraded, grazed, timbered, agriculture, or urban development habitat classes were excluded. These habitat maps were combined with inverse-weighted range maps for each species, whereby species with large ranges were down-weighted and species with smaller ranges were up-weighted. Natural habitat was overlaid with these inverse-range weighted maps summed across all species in the four taxonomic groups to arrive at a final metric of available habitat for endemic species within each taxonomic group.

Habitat for threatened and endangered species. Not all species are equally imperiled at present, nor are they all equally vulnerable to future changes in land use. Thus the amount of habitat available to threatened and endangered species within a country's borders were quantified as an explicit metric in calculations of the biodiversity value of a given land use configuration.

From the species richness data developed, only those species were selected that are listed as "Threatened," "Endangered," or "Critically endangered" in the IUCN Red List of Species. All four taxonomic groupings were summed to create values representing the total number of threatened and endangered species that can be found in each location on the landscape. These values were not weighted as a fraction of the total richness of each taxonomic group. It was assumed instead that all threatened and endangered species are treated as equally important, regardless of how common or rare their broader taxonomic group is globally.

The amount of habitat available for threatened and endangered species was calculated by creating a land cover map that grouped "natural" versus "agriculture, grazed, forested, and built land uses" and tallied the total number of rare and endangered species found in each pixel. Because threatened and endangered species are much less likely to persist in agricultural or built landscapes, all "natural" habitats received a value of 1, and all agricultural and built land uses received a value of 0. However, the study team recognized that there may also be areas recently used for agriculture but are currently degraded and have yet to be restored to their natural habitat. For this reason, it created a mask in which lands are degraded (that is, the potential vegetation map indicates the pixel should be forest, but the pixel is either in grassland or shrubland) and also set these values to 0 in the binary land cover map. For each scenario, the study team multiplied this binary land cover map with the map of potential threatened and endangered species richness. From this emerged location-specific values of how many threatened and endangered species are able to utilize existing natural habitat, which then generated a map in which higher values indicate that preserving natural habitat in that location better protects Red List species.

Key Biodiversity Areas. Key Biodiversity Areas (KBAs) are defined by IUCN as "sites contributing significantly to the global persistence of biodiversity" in terrestrial, freshwater, and marine ecosystems (IUCN 2016). The "Global Standard for the Identification of Key Biodiversity Areas" (IUCN 2016)

articulates the globally agreed-on criteria for the identification of KBAs worldwide. A map of KBAs was laid over the study's map of natural habitat, and the total amount of natural habitat preserved in KBAs was then calculated. The biodiversity data included in these maps were normalized and weighted as described at the end of this section before being included in the optimization analyses.

Habitat in rare ecoregions. Ecoregions are geographically and ecologically defined areas in which the biodiversity of flora, fauna, and ecosystems tend to be distinct. Such areas encompass a spatial scale of biodiversity that is important to protect and can serve as a useful proxy for a country considering its wealth of species, habitat types, and other natural capital assets. Ecoregions have gained significant traction in the conservation literature as an approach to ensure that conservation portfolios protect all species and not just hydrologically diverse regions (Dinerstein et al. 2019; Olson and Dinerstein 2002). Although there are many ecoregion classification schemes, the one used most broadly is the map created by Olson et al. (2001) and recently updated by Dinerstein et al. (2017). This map was validated by Smith et al. (2018) to show that it does, in fact, divide the world into relatively distinct biological communities.

The amount of habitat in rare ecoregions was based on a first calculation of how rare each ecoregion is globally. This was done by taking the inverse of each ecoregion's size. Within each country, the values for the raster representing the rarity of the ecoregion were multiplied by the binary land cover map (which excludes working, degraded, and urban lands).

Forest intactness. It is recognized that simply replacing existing habitat with restored habitat in another location will not necessarily capture the equivalent biodiversity value of the original and the restored habitat. For example, one would expect the intact, undisturbed landscape to have a much higher amount of biodiversity relative to its potential than the restored patch. This is particularly true for forest habitats, which often require years to reach maturity. To account for this, a map of current forest intactness was included (Grantham et al. 2020). This index assigns each pixel globally with a score between 0 and 1 based on the level of forest fragmentation and observed human pressures (such as agricultural development, road networks, and recorded deforestation), with a higher value representing more intact forests. Within each country, pixels that were initially in forest and remained in forest were assigned an intactness score equal to their forest intactness score. Any pixel not currently in forest was assigned a score of 0 (and would remain 0 even if that pixel is reforested). In this way, the optimization selects against conversion of intact forest landscapes.

These six biodiversity indicator maps were then combined by first normalizing them between 0 and 1 (except Key Biodiversity Areas, which were normalized between 0 and 0.5) and then the maximum of the six values was selected as the final value for each pixel.

B.1.3 Agricultural crop production value

Agricultural crop production provides crucial food, feed, fiber, and fuels that support human well-being, provide employment, and generate income that helps boost economies in every country. The impacts of agricultural crop production on other ecosystem benefits and human well-being stem, in part, from foregone land uses. When forest, wetlands, grassland, and other natural habitats are converted into agricultural crop production areas, these areas no longer provide equivalent amounts of biodiversity

habitat, water recharge and filtration, flood retention, carbon storage and sequestration, and other ecosystem services. Another major impact of agricultural production is through the runoff of excess sediment and fertilizer-derived nutrients, with potentially damaging effects on water quality in downstream rivers and coastal regions (Carpenter et al. 1998; Galloway 2003). Air quality can also be negatively affected by agricultural practices such as the particulate matter that arises from fertilization and wind erosion (Bauer, Tsigaridis, and Miller 2016; Hill et al. 2019; Ouyang et al. 2016).

To estimate for every country the value of cropland in every parcel of land, the study team conducted a four-step analytical process to generate crop value maps under the 10 alternative crop management alternatives. It used global information on 10 major crops and the biophysical and socioeconomic factors affecting their value to

- Generate crop yield maps that vary as a function of location, water supply, and source
- Allocate crop mixes to specific locations based on the suitability of growing conditions
- Estimate fertilizer application rates based on predicted yield of each crop in each pixel
- Calculate gross production value and net production value for each crop at each location.

Generating crop yield maps

Crop yield maps for the 10 major global crops (barley, cassava, maize, oil palm, rapeseed, rice, sorghum, soybean, sugarcane, and wheat) were based on harvested yield and area data for each crop across about 20,000 political units from 1974 to 2012 (Ray et al. 2019). These data were normalized so that yield and harvested area matched the national-scale FAOSTAT production data (FAO 2020). The study team then generated estimates for each administrative census unit of harvested yield and area for each crop and its global extent from 2013 to 2018.

Biophysical data affecting crop yields (such as crop-specific temperature and precipitation indexes and soil characteristics) and crop-specific irrigation fractions were then compiled for each administrative census unit to estimate the attainable yield for each crop under different conditions. Attainable yields were modeled using a yield ceiling as a function of biophysical data and whether crops were grown under rainfed or irrigated conditions.

For current ”sustainable management” maps, crop irrigation was changed in those parcels where irrigation is unsustainable based on surface and groundwater supply (Rosa et al. 2019). For those parcels currently growing crops under unsustainable irrigation, the crop yields were changed to those attainable under rainfed conditions, and country average yield gaps were applied (World Bank 2020).

Allocating crops to specific locations based on suitability of growing conditions

Suitability of growing conditions for each crop in each country were modeled as a function of landscape slope, weather conditions (such as temperature, precipitation, and growing degree days), soils, and sustainability of irrigation. Slopes suitable for crop agriculture were determined by computing the average slopes on which agriculture is practiced in each country. A parcel of land was considered not suitable for agriculture on slopes exceeding the 95th percentile of slopes in crop production in a country or on a slope greater than 10 percent (the point at which tractors can no longer be used and mechanization becomes more difficult), whichever was higher.

In addition to slopes, biophysical suitability for each crop in each country was defined based on climate and soil quality attributes. Climatic suitability was quantified using a method analogous to ecological niche modeling. The conditions under which a crop is observed to be grown are assumed to be suitable, subject to data quality considerations. Soil quality suitability was determined from Zabel, Putzenlechner, and Mauser (2014).

Crops were allocated to each parcel under different agricultural production scenarios—extensification versus intensification, rainfed versus irrigated.

Estimating site- and crop-specific fertilizer application rates and yield

Fertilizer application rates for each crop in each location were estimated using 2000 fertilizer application data (Mueller et al. 2012) and crop data (Monfreda, Ramankutty, and Foley 2008). A statistical regression model related fertilizer application rates to yield in 2000, and the model was then used to estimate fertilizer application rates required to achieve average crop yields for each country observed in 2015.

Calculating total production costs and value for each crop at each location

Gross income from crop production was estimated for each crop and parcel as total production (metric tons) multiplied by producer price. Production was calculated as yield multiplied by harvested area for each of the 10 crops in each pixel. The average producer price for each crop and country based on Food and Agriculture Organization (FAO) data was used for the calculations (FAO 2020). In this analysis, crop prices were taken as exogenous—that is, prices do not change with changes in the supply of crops due to changes in land use or land management. With large changes in crop production, one would expect prices to adjust to meet demand. Equilibrium prices were estimated using a computable general equilibrium model such as that of the Global Trade Analysis Project (GTAP)—Hertel (1997). Such an approach was recently adopted for a related project described in the World Bank report *The Economic Case for Nature* (Johnson et al. 2021).

The study team calculated transport costs based on travel time to the nearest city from farm fields (Weiss et al. 2018), the minimum wage for truck drivers (International Labour Organization), a fuel efficiency of 0.4 liters per kilometer, the cost of diesel fuel (World Bank 2020), and the assumption that each truck carries 15 metric tons of crop.

The GTAP 10 Data Base (Aguiar et al. 2019) was used to convert gross returns to net returns for agricultural crops. The same procedure was used for forestry and grazing. The GTAP 10 Data Base provides information on 25 factors of production for 65 economic sectors in 141 regions.

Table B.2 shows how the study team matched GTAP sectors to the 10 agricultural crops, forestry, and grazing activities.

Table B.2 Matchups of GTAP sectors and Landscape Efficiency Scores economic activity

GTAP sector description	NCI economic activity
Rice	Rice
Wheat	Wheat
Maize (corn), sorghum, barley, rye, oats, millet, other cereals	Barley, maize, sorghum
Vegetables, fruit and nuts, edible roots and tubers with high starch or inulin content, pulses (dried leguminous vegetables)	Cassava
Oil seeds and oleaginous fruit	Oil palm, soybean, rapeseed
Sugar crops	Sugarcane
Bovine cattle, sheep and goats, horses	Grazing
Forestry	Forestry

Source: Original table for this publication.
Note: GTAP = Global Trade Analysis Project.

The factors of production include types of land (18 agroecological zones, AEZs), five types of labor (such as clerks and agricultural and unskilled labor), and two types of capital (capital and natural capital). The factor share for land (18 AEZs) was multiplied by the gross returns to generate an estimate of net returns. This method nets out costs for labor, produced capital, and other manmade inputs. The GTAP 10 Data Base has data for most large countries, but it groups smaller countries into regions. For example, Bangladesh, India, Nepal, Pakistan, and Sri Lanka are reported separately, whereas Afghanistan, Bhutan, and Maldives are combined into a region called "Rest of South Asia." Individual country data were used when available in GTAP and regional data for other countries.

B.1.4 Livestock grazing production value

The value of meat production from beef cattle was used as an estimate of grazing value on every parcel of land for every country. The study team conducted a four-step process to generate grazing value maps at 10 square kilometer (km^2) resolution following methods used by Castonguay et al. (2022). First, information on meat production and biophysical and socioeconomic factors affecting production based on the ORCHIDEE GM model (Chang et al. 2016) were used to generate a mean annual grazed biomass value over a 30-year period (1987–2016) for each 10 km^2 grid cell. The highest sustainable grazed biomass value for each cell was selected from among the three modeled grazing intensities (25 percent, 37.5 percent, and 50 percent). The resulting highest sustainable grazing intensity is consistent with previous work such as that by Fetzel et al. (2017), where grazing intensity is higher in colder regions and lower in arid and tropical regions. Meat production (kilograms/hectare) for each cell was calculated

based on the amount of biomass multiplied by the energy in grass, the liveweight gain factor, and the dressing factor (see table B.3 for parameter values and data sources).

Second, the study team calculated methane emissions measured in terms of CO_2 equivalents (kilograms of CO_2eq per hectare per kilogram of beef, or kg CO_2eq/ha/kg) for each pixel of grazing land as a function of grazed biomass and a methane emissions conversion factor (kg CO_2 eq/ha), manure as a function of grazed biomass and a manure emissions factor (kg CO_2 eq/ha), and transportation (kg CO_2 eq/ha), which depends on travel time to the nearest urban center, average speed, fuel efficiency, and a road emissions factor (see table B.3 for parameter values and data sources). Methane emissions based on livestock density were aggregated over 20 years and were subtracted from carbon emissions.

Table B.3 Parameters used in estimating livestock production value

Parameter	Description	Value	Unit	Source
BM_i	Grazed biomass	—	t/ha	Chang et al. (2016)
ME_{rz}	Energy in grass	—	MJ/t DM	Herrero et al. (2013)
LW_{rz}	Liveweight gain conversion factor	—	kg/MJ	Herrero et al. (2013)
Dressing	Dressing percentage	60	%	FAO (2021a)
$MethEF_{rz}$	Methane emission factor	—	kg CO_2 eq/t DM	Herrero et al. (2013)
$ManEF_{rz}$	Manure emission factor	—	kg CO_2 eq/t DM	Herrero et al. (2013)
Capacity	Truck payload capacity	15,000	kg	Delgado et al. (2016)
$Travel_i$	Travel time to nearest urban centre (50,000 inhabitants or more)	—	Minutes	Weiss et al. (2018)
Speed	Average speed	1	km/min	Delgado et al. (2016)
FE	Fuel efficiency	0.4	l/km	Waldron et al. (2006)
$Diesel_c$	Cost of diesel	—	US$/l	GIZ (2019)
REF	Road emission factor	2.7	kg CO_2 eq/l	Waldron et al. (2006)

Source: Original table for this publication.

Note: — = not available; kg CO_2 eq/l= kilogram CO_2 equivalent/liter; kg CO_2 eq/t DM= kilogram of CO_2 equivalent/tonne; kg/MJ= kilogram/megajoule; l/km=liter per kilometer; MJ/t DM= megajoule/tonne dry matter; t/ha = tonnes/hectare; FAO = Food and Agriculture Organization of the United Nations.

Third, meat production (kg/ha) in each grid cell was multiplied by the price of meat ($/kg) for each country, using a 10-year average price for cattle meat (2006–2015) as reported by FAO producer prices (FAO 2021b). Transport costs (US$/ha/kg of beef) to production in each pixel were subtracted. The costs were based on travel time to the nearest city from the pixel (Weiss et al. 2018), the minimum wage for truck drivers (ILO 2021), a fuel efficiency of 0.4 liters per kilometer (l/km) (Delgado et al. 2016), the cost of diesel fuel (World Bank 2020), and the assumption that each truck carries 15 tons.

Finally, the potential meat production costs were calculated using the method just described for agricultural crops. Production costs were subtracted from gross revenue to determine net revenue from meat production.

Where needed, gaps were filled in the potential beef layer by using a nonlinear regression with net primary productivity (NPP; MOD17A3 v055) as the independent variable and grazed biomass as the dependent variable, so that

$$Biomass = \frac{a \times NPP}{b + NPP} \quad . \qquad \text{(B.1)}$$

The three different grazing intensities (25 percent, 37.5 percent, and 50 percent), and the highest grazed biomass value was selected, as earlier. One regression was run for each grazing intensity–fertilizer scenario to first fill the gaps for each scenario and then to create a layer of "best-grazed biomass" by selecting the highest biomass value across the three grazing intensities.

B.1.5 Forestry production value

Forestry yield for each parcel and scenario was estimated by first using a global forest vegetation map generated by the MC2 dynamic global vegetation model from Kim et al. (2017). Forest biomass for each vegetation type was estimated using a growth function based on the empirical equation from Favero et al. (2020),

$$V_{a,t}^{i}\left(m_{a,t}^{i}\right) = h \times [\exp\left(\delta^{i} - \frac{\pi}{a}\right)] \quad , \qquad \text{(B.2)}$$

where $V^{i}_{a,t}$ is yield in cubic meter per hectare; h is tree stocking density that depends on management intensity; $\boldsymbol{\delta}$ and π are species-dependent growth parameters; and a is tree age in decades.
Timber growth functions were specified for each type of vegetation in each of 16 global timber regions (from Tian et al. 2016). These growth functions were applied to generate potential forest yield for each parcel and scenario. Some regions do not have sufficient information to estimate distinct forest types (for example, the African continent had one type). In these areas, 15-year average net primary productivity (NPP) was used to scale annual biomass yield, and the nearest neighborhood convolutions technique was used to fill the gap of the potential annual biomass yield. Gaps in the potential yield map were filled-in based on a nearest neighbor approximation with a Gaussian kernel of 25 kilometers. Forestry yields within each global timber region were then scaled linearly using net primary productivity, so that a pixel with twice the average NPP will have twice the timber returns, while a pixel with half the average NPP will have 50 percent of the timber returns.

From potential forest yield, monetary returns were calculated by multiplying harvest volumes by regional log prices (Siikamäki and Santiago-Ávila 2014). Transportation costs, calculated using the same method as for crop transportation cost (except the truckload is assumed to be 40 square meters per truck and volume rather than weight assumed), were then subtracted. For countries with missing log prices, the nearest neighborhood analysis was used to fill the gap. Net monetary return from managed forestry was calculated by subtracting transportation cost from monetary return. The same method was used to calculate production costs as described earlier for agricultural crops to convert from gross production value to net production value.

B.1.6 Exposure to nitrates in drinking water

Excess nitrogen concentrations in ground and surface water is the result of (1) excess nitrogen application from farming and livestock; (2) insufficient natural capital and poor management resulting in

excess export of nitrogen to ground and surface water bodies; and (3) point sources of nitrogen such as insufficiently treated urban wastewater. Land use change, in particular the conversion to agricultural lands, modifies the natural nutrient cycle. Nitrogen loads are likely to increase under scenarios with intensified agriculture—that is, expansion of agricultural area or heavier nitrogen application. When it rains or snows, water flows over the landscape carrying pollutants from these sources into streams, rivers, lakes, groundwater bodies, and eventually the ocean. The health or well-being of people is directly affected (Keeler et al. 2012), as well as the aquatic ecosystems that have a limited capacity to adapt to these nutrient loads. One way to reduce nonpoint source pollution is to reduce the amount of anthropogenic inputs (that is, fertilizer management). In addition, ecosystems can provide a purification service by retaining or degrading pollutants before they enter the stream. For example, vegetation can remove pollutants by storing them in tissue or releasing them back to the environment in another form. Soils can also store and trap some soluble pollutants. Wetlands can slow flow long enough for pollutants to be taken up by vegetation or, in the case of nitrogen, to be returned to the atmosphere. Riparian vegetation is particularly important in this regard; it often serves as a last barrier to block nutrient runoff from upland areas before it enters a stream.

Application of higher quantities of nitrogen during agricultural intensification or the loss of natural vegetation from extensification of agricultural and other development can increase nitrogen in water bodies and drinking water, which is the focus in this report. Excess nitrogen also has wide-ranging impacts on air pollution, thereby affecting human health, climate change and stratospheric ozone depletion, eutrophication and other forms of water pollution other than impacts on drinking water, and biodiversity loss. These impacts contribute directly and indirectly to a number of human health concerns, including respiratory ailments and cardiac disease, as well as impacts on ecosystem services and biodiversity that are not factored here. However, the model used in this report only captures one such impact, which is colorectal cancer.

Although there is evidence that nitrate is linked to human health outcomes—such as “blue baby syndrome” (methemoglobinemia), adverse birth outcomes (low birth weight, preterm birth, and neural tube defects), and several forms of cancer—nitrate itself is generally not toxic. However, when ingested it can become nitrite, which reacts with hemoglobin to cause methemoglobinemia or to form N-nitroso compounds, which are carcinogenic. These health impacts have led to global and national standards for nitrogen in drinking water. Temkin et al. (2019) recently estimated a dose–response relationship between exposure to nitrate in drinking water and colorectal cancer. Such a relationship presents the possibility of incorporating an estimated health impact based on changes in the amount and location of natural ecosystems, agriculture, and agricultural management practices. The focus here is on the nitrate concentration in drinking water (after considering country-specific rates of drinking water origins from surface and groundwater) in order to not discount health outcomes that cannot be modeled.

Model process and endpoints

This model links (1) nitrogen loads derived from the InVEST Nutrient Delivery Ratio (NDR) model to (2) nitrate concentrations in surface and groundwater and (3) nitrogen concentrations in surface and groundwater to colorectal cancer incidence as a function of nitrogen concentrations in drinking water sources.

An alternative estimate of the impact of excess nitrogen in water supply is to quantify the nitrogen abatement costs to treat drinking water to World Health Organization (WHO) standards under different land use scenarios. However, the WHO standards for drinking water treatment are based on the very high safe thresholds for blue baby syndrome and not cancer impacts, and so will be exceeded in very few places. Thus abatement cost measures are not sensitive to changes in natural capital and the study team did not integrate abatement costs as an end metric in the landscape efficiency score.

Although drinking water nitrate has been associated with other adverse health consequences (such as blue baby syndrome and adverse birth outcomes), no general dose–response relationship or even generalized links between health outcomes and particular levels of exposure have been established for these other effects. This model therefore captures only an illustrative, lower estimate for the negative health effects of nitrate in drinking water based on the available data linking to colorectal cancer rates. Globally, there are an estimated 15,000–75,000 nitrate-attributable colorectal cancer cases per year (Temkin et al. 2019). Similarly, no methods currently exist to quantitatively link nitrogen concentrations, aquatic ecosystems, and associated services (such as impacts on fisheries) on a global scale. These impacts were thus also omitted from this study's estimates of nutrient impacts.

Modeling nitrogen loads using the InVEST NDR model

The InVEST Nutrient Delivery Ratio model was used to model nitrate loads in water sources as a function of changes in land use/land cover (Sharp et al. 2020). In a first step, the NDR model quantified the delivery of nitrogen from agriculture and other diffuse LU/LC-based sources to rivers (nitrogen export) as a function of nitrogen fertilizer application rates and background rates of nitrogen loading from nonagricultural land covers and the capacity for nitrogen retention by vegetation on the landscape. The model uses a simple mass balance approach, describing the movement of a mass of nutrients through space. Unlike more detailed nutrient models, it does not represent nutrient cycle dynamics, but rather represents the long-term, steady-state flow of nutrients through empirical relationships. Sources of nutrients across the landscape, also called nutrient loads, are determined based on a LU/LC map and associated loading rates as well as spatially explicit fertilizer application rates (corresponding to the rates used to model crop production). In a second step, delivery factors are computed for each parcel based on the properties of pixels belonging to the same flow path (in particular, their slope and the retention efficiency of the land use). Thus the model captures two mechanisms relevant for nutrient exports to streams: (1) spatial variability in application and (2) spatial variability and vegetation impacts on export. Each pixel's value for nitrogen export reflects its contribution to the total amount of nitrogen reaching the stream.

Nitrogen fertilizer application rates are derived by extrapolating observed global application rates for intensive and extensive cropping practices for the top 10 crops by harvested area (barley, maize, oil palm, potato, rice, soy, sugar beet, sugarcane, sunflower, wheat), using a weighted average based on their proportional area. It is assumed that the crop compositions will remain constant in current agroclimatic zones. For extensification, current average nitrogen fertilizer application rates are applied to each 5 arc min grid cell; for intensification, the nitrogen application rates required to close yield gaps are set (Mueller et al. 2012). Background rates of nitrogen loading and nitrogen retention coefficients are set according to land cover type (Chaplin-Kramer et al. 2019). The model uses long-term average

climate conditions for precipitation runoff (Fick and Hijmans 2017) and is routed using a Digital Elevation Model at 90-meter resolution (NASA STRM 2013).

Modeling nitrogen concentrations in surface and groundwater

The next step is to use the NDR model outputs to model the resulting nitrogen concentration in water bodies on which nitrate-attributable cancer risks depend. In a recent study, the World Bank compiled a list of available observations of surface and groundwater quality, including concentrations of nitrogen compounds (Damania et al. 2019). These observations cover a significant area of the globe (though with a spatial bias) and a considerable timespan. The empirical observations allowed the team to build data-driven models that link environmental covariates of climate, hydrology, hydrogeology, and urban extent with nitrate concentrations in surface and groundwater (for a list of covariates, see Damania et al. 2019 technical appendix [https://openknowledge.worldbank.org/bitstream/handle/10986/32245/211459App.pdf] or Desbureaux et al. 2022). The team updated this approach by adding the outputs of the NDR model (nitrogen delivery to streams in in kilograms per year) to other environmental covariates to train a machine learning model that predicts nitrate concentrations (mass/volume) in surface and groundwater from modeled nitrogen export and environmental covariates with a global 10 × 10 square klometer resolution. The machine learning model thus links observed NO_X-N data, environmental covariates, and InVEST NDR outputs to predict NO_X-N concentrations in surface and groundwater.

B.2 Sustainability

Sustainable outcomes for all solutions along the efficiency frontier and for the analysis of the current situation were modeled. Sustainability was incorporated into the analysis by assuming that whatever land use and land management option was designated for a pixel does not change through time. These LU-LM options were constrained to not deplete natural capital. The constraint ruling out depletion of natural capital came into play in modeling grazing intensity and water use for irrigation. For grazing, animal density was selected based on the amount that maximizes biomass production and maintains at least 25 percent of standing biomass after grazing. For water use, irrigation was not allowed in areas where such irrigation is supplied by the unsustainable mining of groundwater aquifers (Rosa et al. 2019). In these areas, any agricultural crop production must be rainfed and not irrigated. However, one area in which the data are inadequate to model depletion of natural capital is soil degradation from unsustainable agricultural practices.

B.3 Scenarios of land use and land management

Thirteen land use and land management alternatives that can be applied to any given land were modeled. Each different LU-LM alternative for each parcel was scored using the models described earlier for agricultural crops, grazing, and forestry production, as well as biodiversity, greenhouse gas storage and emissions reduction, and nitrate concentration in drinking water. The optimization procedure (described shortly) chooses among the 13 LU-LM alternatives for each land parcel to achieve outcomes along the efficiency frontier.

Land use and land management alternatives

There are 13 land use and land management alternatives in addition to the sustainable current land use: restoration, forestry, grazing, and 10 crop production alternatives.

For protected areas as denoted by the IUCN, the addition of cropland, grazing, or forestry into any IUCN classes I–IV protected areas was not allowed. To generate the "sustainable current" scenario, existing cropland was removed from land in IUCN classes I–IV and VI. Current uses (but no expansion) were allowed on IUCN class V. Grazing and forestry expansion, but not cropland expansion, was allowed in IUCN class VI.

Sustainable current. The European Space Agency land use/land cover map was used as the current landscape map for every country (ESA 2019), except those areas in which the current land use is unsustainably irrigated cropland (that is, withdrawals exceed recharge— Rosa et al. 2019) and has been converted to rainfed cropland. Cropland was removed from certain IUCN-designated protected areas.

Restoration. In this alternative, all nonurban pixels were converted to their potential vegetation as defined by the ESA land cover map (ESA 2019). Modeling the effects of restoration on landscapes in each country requires identifying a logical habitat type that will result from restoration activities in each location. To determine what land cover classification could be restored from a parcel that is currently under agricultural crop production, grazing, or forestry, the study team used a two-step process. In the first step, it restricted the potential vegetation classes to which a parcel can transition using a map of global biomes. In this way, it was able to ensure that errors in remote sensing data or human activity (for example, the conversion of natural forests to managed grassland or the conversion of natural grassland to plantation forests) did not result in inappropriate habitat types under restoration. In the second step, it used a spatial algorithm based on Gaussian decay functions with simple rules to select the most likely natural land class to which a current agricultural cell will revert after constraining it based on the biome it occupies.

Crop production alternatives (10). The cropland scenarios consist of combinations of cropland management choices:

- Intensification versus current practices
- Extensification versus current crop extent
- Irrigated versus rainfed
- With or without best management practices.

Agricultural best management practices were represented by converting 10 percent of the agricultural parcel (pixel) to native habitat and restoring riparian buffers (the pixels immediately adjacent to streams, as delineated in the hydrological modeling) according to their native/potential natural vegetation classes (see *restoration*). This resulted in different areas of natural habitat within parcels, depending on the density of the stream network.

The intensification of crop agriculture was split into irrigated and rainfed parcels, depending on the sustainability of water for irrigation (Rosa et al. 2019) and the application of fertilizer required to close

yield gaps for rainfed or irrigated production, respectively. For BMPs, the fertilizer application rate was 90 percent of the respective rate for rainfed or irrigated intensified crop production; BMPs were only applied to intensified agricultural parcels (not to parcels for current agricultural practices).

The 10 crop production alternatives are summarized in table B.4. Two alternatives use current production methods, and eight use intensified production methods.

Table B.4 Alternative crop production management

	Intensity		Extent		Water management		BMPs	
Crop production alternative	Current	Yield gap closure	Current	Maximum	Rainfed	Irrigated	No	Yes
Sustainable current	X		X		X		X	
Expanded current	X			X	X		X	
Intensified production methods								
Current extent, rainfed, without BMPs		X	X		X		X	
Current extent, rainfed, with BMPs		X	X		X			X
Current extent, irrigated, without BMPs		X	X			X	X	
Current extent, irrigated, with BMPs		X	X			X		X
Expanded extent, rainfed, without BMPs		X		X	X		X	
Expanded extent, rainfed, without BMPs		X		X	X			X
Expanded extent, irrigated, without BMPs		X		X		X	X	
Expanded extent, irrigated, with BMPs		X		X		X		X

Source: Original table for this publication.
Note: BMPs = best management practices.

For all cropland management alternatives, several suitability rules were applied:

- *Sustainable irrigation.* In all scenarios involving irrigation, irrigation was allowed only where it was considered sustainable (Rosa et al. 2019). In areas where irrigation was unsustainable, crop management alternatives were restricted to include only rainfed cropland.
- *Slope threshold.* Expansion of intensified cropland was allowed only into pixels with an average slope of less than 10 percent. Pixels steeper than this threshold remained in their current state.
- *Crop suitability*. Each specific crop type was constrained by its suitability in climate, slope, and soil characteristics and was only able to expand to suitable pixels. In expansion scenarios, cropland was only expanded into pixels suitable for at least one crop type. Possible extents for

irrigated and rainfed crop production were defined according to climate (that is, growing degree days and precipitation suitability for the top 10 crops). Suitability of a parcel for crop production was also defined based on soil type characteristics (Zabel, Putzenlechner, and Mauser 2014) and the slope of the parcel. Agricultural expansion (using "current practices") was not allowed as a transition in the optimization analysis on slopes exceeding the 95th percentile of slopes in that country or on a slope greater than 10 percent (the point at which tractors can no longer be used and mechanization becomes more difficult), whichever was higher. Intensified agricultural expansion was not allowed on slopes exceeding 10 percent.

- *Grazing*. Grazing was allowed in all suitable pixels as defined by the grazing production model but was not allowed in IUCN class I–IV protected areas.
- *Forestry*. Forestry was allowed in all suitable pixels as defined by the forestry production model but was not allowed in IUCN class I–IV protected areas.

B.4 Transition costs

Transitions between land uses typically require an upfront investment cost. For example, converting land into agricultural crop fields from natural vegetation entails clearing costs and crop establishment costs. Restoring agricultural cropland to natural habitat typically requires replanting and other restoration costs. In areas without established irrigation, transitioning to irrigated agriculture requires investment to install irrigation infrastructure. Table B.5 describes the costs that apply to various potential transitions.

Table B.5 Transition costs included in scenarios

From \ To	Natural habitat	Current agriculture	Forestry	Grazing	Intensive agriculture, rainfed	Intensive agriculture, irrigated
Natural habitat	0	Cost of clearing land and establishing crops	Cost of establishing forest (will vary by habitat type)	Cost of clearing land	Cost of clearing land, establishing crops, and improvements for intensification	Cost of clearing land, establishing crops, and improvements for intensification and irrigation
Current agriculture	Restoration costs (will vary by habitat type)	0	Cost of establishing forest	0	Costs of improvements for intensification	Costs of improvements for intensification and irrigation

From \ To	Natural habitat	Current agriculture	Forestry	Grazing	Intensive agriculture, rainfed	Intensive agriculture, irrigated
Forestry	Restoration costs (will vary by habitat type)	Cost of clearing land and establishing crops	0	Cost of clearing land	Cost of clearing land, establishing crops, and improvements for intensification	Cost of clearing land, establishing crops, and improvements for intensification and irrigation
Grazing	Restoration costs (will vary by habitat type)	Cost of establishing crops		0	Cost of establishing crops and improvements for intensification	Cost of establishing crops and improvements for intensification and irrigation
Intensive agriculture, rainfed	n.a.	n.a.	n.a.	n.a.	0	n.a.
Intensive agriculture, irrigated	n.a.	n.a.	n.a.	n.a.	n.a.	0

Source: Original table for this publication.
Note: n.a. = not applicable.

Restoration costs

The independent study Economics of Ecosystems and Biodiversity (TEEB) has estimated the costs of restoring natural habitat by habitat type (TEEB 2009). TEEB reports the "typical" costs per hectare (table B.6). The study team scaled costs per hectare to countries based on relative wages (ILO 2021). Each country's labor costs were divided by the median labor cost globally, and then that scaling factor was multiplied by these restoration costs per hectare to estimate a country-specific cost of restoration. These scaled costs were comparable to country- and habitat-specific costs from Bayraktarov et al. (2016), the only global meta-analysis of restoration costs for marine and coastal habitats. The list of average hourly wages for skilled fishery, agricultural, and forestry industries compiled by the International Labour Organization (ILO) provided data for 48 countries. If data were not available for a country, the average of the subregion was used. If data for none of the counties in a subregion were available, the data for the country were adjusted based on the minimum wage database of ILO (2021).

To weight by labor differential, the study team took the average or median labor cost globally from ILO data and then divided each country's (or region's) labor cost by it. It then multiplied that scaling factor by these global costs to get the country- (or region-) specific cost of restoration.

Table B.6 Estimate of restoration costs, by habitat type

Habitat type	Restoration cost estimate (US$/hectare)
Inland wetlands	33,000
Lakes/rivers	4,000
Tropical forests	3,450
Other forests	2,390
Woodlands/shrubland	990
Grasslands	260

Source: TEEB 2009.

Land clearing and land establishment cost

Estimates of land clearing costs were based on the assumption that land clearing would be carried out by machine mulching of existing vegetation. Cost estimates were based on a vertical shaft mulcher. For land clearing, the study team estimated the cost of the vertical shaft mulcher, the operation cost, and the maintenance cost using Iowa State University's guide for the cost of owning agricultural machinery. The cost of the machine over its useful life was estimated by deducting salvage value from list price. Operation cost included fuel cost and labor cost. Fuel and labor costs vary by geographic location. Fuel cost per liter was collected from the World Bank's World Development Indicators (WDI) database. For labor costs, the study team used the International Labour Organization database (ILO 2021). The list of average hourly wages for skilled fishery, agricultural, and forestry industries compiled by ILO provided data for 48 countries. If data were not available for a country, the average of the subregion was used. If data for none of the counties in a subregion were available, the data for the country were adjusted based on the minimum wage database of ILO (ILO 2021).

Three field operations are required to convert pastureland to agricultural crop production. Illinois State University provided the cost of these three operations. Using this guide and adjusting for fuel and labor costs for all the countries, the study team estimated the cost of land establishment.

Irrigation costs

The International Water Management Institute provided irrigation setup costs for subregions. The study team used the value for successful projects, which are defined as having a greater than 10 percent economic internal rate of return at project completion.

Annualizing transition costs

All transition costs were annualized assuming a 20-year amortization with a 3 percent discount rate.

B.5 Optimization

An optimization analysis was used to construct the efficiency frontier, which shows the range of Pareto-efficient combinations of sustainable environmental and economic objectives that can be attained through different land use and land management choices. The optimization analysis used a discrete choice (integer programming) model in which a land use decision is made for each land parcel in a given country. A land parcel is a larger spatial unit that contains multiple smaller land units (pixels). The scale of pixels is defined by the resolution of spatially explicit data—in this analysis the scale was 300 square meters. A parcel's score for an objective is the sum of the values of its constituent pixels. In the optimization analysis, a parcel can be assigned to one of several alternative land use and land management options. Some pixels were precluded from certain land uses or management options (as described earlier). For example, agriculture was excluded from some areas because the land is unsuitable for crop production either because of poor soil or steep slopes, or because the land is in a protected area. Each parcel was given a score for each objective under each land use and land management alternative according to the models for biodiversity, carbon storage, agricultural crop production, grazing, forestry, and drinking water quality. The optimization procedure is as follows:

- Evaluate each objective (*o*) in each parcel (*p*) for each LU-LM alternative (*m*). Doing so generates the value for each objective on each parcel for each LU-LM alternative: v_{mp}^{o}.
- Run a sequence of optimizations with weights, w_o , assigned to each objective, $0 \leq w_0 \leq 1$, $\sum_{\square} w_0 = 1$, and solve the optimization problem

$$\sum_m \sum_p x_{mp} w_o v_{mp}^{o}, \qquad \text{(B.3)}$$

  where $x_{mp} \in [0,1]$ and $\sum_m x_{mp} = 1$ for each *p*.
- These optimizations identify the optimal landscape, consisting of the optimal decisions (choice of management option) for each parcel, given w_o. The collection of these individual optimizations with different weights outlines the frontier.

B.6 A general equilibrium model of reallocation gains from correcting externalities

What are the aggregate implications of recognizing the social cost of carbon in different countries? To answer this question, the study team considered a general equilibrium model of agriculture featuring environmental externalities. Carbon sequestration benefits are modeled as a parameter that has a positive impact in the welfare function. A stylized feature in the model is that natural capital such as forests provides a positive externality in the welfare function when the value of sequestration is recognized. As the importance of the land cover is recognized by the social planner, land will be allocated to nature for environmental services (sequestration) of which the benefits are often neglected in the economy.

Agriculture sector

The stylized production unit in agriculture is a farm that requires land and labor as inputs described by a constant return to scale technology. Output in agriculture Y_a requires the inputs of land L_a and labor N, where $0 < \gamma < 1$ denotes the relative importance of land in producing food, and A_a is agricultural total factor productivity (TFP)[1]:

$$Y_a = A_a L_a^{\gamma} N^{1-\gamma} \tag{B.4}$$

$$\pi = A_a L_a^{\gamma} N^{1-\gamma} - qL_a - wN \tag{B.5}$$

$$\frac{d\pi}{dL_a} \Rightarrow q = \gamma A_a L_a^{\gamma-1} N^{1-\gamma} \tag{B.6}$$

$$\frac{d\pi}{dN} \Rightarrow w = (1-\gamma) A_a L_a^{\gamma} N^{-\gamma} = w \tag{B.7}$$

$$\frac{w}{q} = \frac{1-\gamma}{\gamma} \frac{L_a}{N}. \tag{B.8}$$

Agricultural land is used for production purposes; environmental land cover is used for carbon sequestration; and "unusable land" is land that is unsuited for either purpose and cannot be used for production or sequestration purposes (for example, deserts). The land market clearing condition represents the land inputs as shares, so that

$$1 = L_a + L_e + L_n. \tag{B.9}$$

Social planner's problem

A representative household (social planner) chooses to allocate land to the agriculture sector or to environmental sequestration to maximize welfare. The household budget constraint is

$$A_a L_a^{\gamma} N^{1-\gamma} = Y_a = c_a = qL_a + wN. \tag{B.10}$$

Welfare depends on the amount of agricultural goods being consumed, and sequestration benefits from land cover. Aside from land input, environmental benefits from sequestration depend on the carbon sequestration efficiency A_e, the social cost of carbon (carbon taxes) δ, and the preference of environmental services over agricultural consumption ϕ (green preference). Because this is a closed economy, the benefits from consumption depend on the amount of agricultural production:

$$W = \underbrace{\delta\phi \log(A_e L_e)}_{Environmental\ Benefits} + \underbrace{(1-\phi) \log(c_a)}_{Consumption}$$

[1] The study team abstracted from capital and intermediate inputs, both of which are known to magnify the productivity and income implications and are discussed in detail in the literature (Adamopoulos and Restuccia 2014; Restuccia, Yang, and Zhu 2008).

$$W = \delta\phi\ log(A_e(1 - L_a - L_n)) + (1 - \phi)\ log\ (A_a L_a^{\gamma} N^{1-\gamma})$$

$$\frac{dW}{dL_a} \Rightarrow \frac{\delta\phi}{1-L_a-L_n} = \frac{\gamma(1-\phi)}{L_a} \Rightarrow \frac{\delta\phi}{\gamma(1-\phi)} = \frac{1-L_a-L_n}{L_a}. \quad \text{(B.11)}$$

Maximizing for the distribution of land and solving for L_a gives

$$L_a = (1 - L_n)\frac{\gamma(1-\phi)}{\delta\phi + \gamma(1-\phi)}. \quad \text{(B.12)}$$

From equation (B.8), L_a depends negatively on ϕ, δ and positively on γ assuming ϕ or δ is not 0. The social planner's land allocation is restricted by the share of bare area L_n. One assumption of the model is that land that can be farmed can be reforested but cannot be expanded to the unusable area. Therefore, $L_a \to (1 - L_n)$, when $\phi \to 0$ or when $\delta \to 0$. In the model, ϕ could be interpreted as either a green preference parameter or the costs of switching land between environment and agriculture.

Calibration

Two different scenarios were compared: a world in which the social cost of carbon is not recognized and thus without any carbon taxes and a world in which the carbon tax is imposed and thus the environmental benefits of land covers are recognized. To calibrate a benchmark economy that is a world without carbon taxes, it was assumed that the social cost of carbon is close to 0. In the counterfactual experiment, the social planner recognizes the sequestration benefits of environmental land covers, and δ is normalized to 1.

The benchmark economy was compared to the counterfactual scenario for 144 countries. Each country differs in three country-specific parameters (A_a, γ, L_n), so the changes in welfare between the countries can be compared when the sequestration benefits of land cover is recognized from the model.

Parameterization

The following country-specific parameters are heterogeneous between each country:

- $\boldsymbol{A_a}$ = agricultural TFP and is represented by actual-to-potential yield ratio from Global Agro-Ecological Zones (GAEZ).
- $\boldsymbol{\gamma}$ = land elasticity in agricultural production and was assigned based on agricultural income shares.
- $\boldsymbol{L_n}$ = share of "unusable" land and is represented by Organisation for Economic Co-operation and Development (OECD) data on bare area.

Without loss of generality, labor input was set at *N* = 1, and the price of agricultural goods was normalized to 1. Similar to Adamopoulos and Retuccia (2020), agricultural TFP $\boldsymbol{A_a}$ was represented by the actual-to-potential yield ratio from GAEZ and weighted by each yield ratio group. When $A_a = 100$,

agricultural goods are produced at their full potential. The green preference parameter ϕ was chosen at 0.74 to reconcile the global environmental land shares to those reported by OECD.[2]

Span-of-control parameter γ was estimated using growth accounting from other sources. There is some consensus that the labor share in agriculture should be about one-half for most countries (Gollin, Lagakos, and Waugh 2014). The remaining half is normally represented by the sum of capital and land shares. This model allows only for land and labor, and so the computation for capital is excluded. Both Valentinyi and Herrendorf (2008) and Adamopoulos and Restuccia (2014) use a labor share of 0.46 with US data and a land income share of 0.18 with US data. Therefore, excluding the computation for capital, for the high-income countries in the model was assigned 0.28. Generally, the land income share in agriculture is larger in poor countries (Santaeulalia-Llopis and Restuccia 2014). For low-income countries, the estimate from Restuccia and Santaeulalia-Llopis (2015) was used in which the land income share is double the capital income share and set at γ = 0.44 for low-income countries. For upper-middle-income and lower-middle-income countries, γ was assigned 0.33 and 0.38, respectively, to maintain a similar range between the income groups. Table B.7 gives the full set of parameters used.

Table B.7 Parameterization

Parameters	Value		Target
Technological parameters	*Benchmark*	*Counterfactual*	
A_a	Country-specific	Country-specific	Actual-to-potential yield ratio
A_e	100	100	Normalization
γ	Country-specific	Country-specific	Agricultural land income share
Preference parameters			
ϕ	0.74	0.74	Global land cover share
δ	0	1	Normalization
L_n	Country-specific	Country-specific	Share of "unusable land"
Labor endowment			
N	1	1	Normalization

Source: Original table for this publication.

Results

Table B.8 shows the aggregate welfare of each country group before and after recognition of the social cost of carbon. The country-specific parameters are agricultural TFP, relative importance of land in agricultural production, and share of bare area. For the aggregate results, W_{BE} is the welfare in the benchmark economy; W_{EXT} is the welfare in the experiment with externalities; $W_{BE}Rank$ and $W_{EXT}Rank$ are the ranks of the regions; and $W(\Delta\ \%)$ is the percentage increase in welfare from the benchmark to the experiment. In table B.8, country groups that have lower agricultural TFP, lower γ,

[2] $\phi = \frac{Global\ land\ cover}{Global\ land\ cover + Global\ agricultural\ land}$. For each country, land shares from OECD stats are multiplied with land size from World Bank data for 2019 to estimate global land cover and global agricultural land. L_a = crop land; L_e = tree cover, grassland, wetland, shrubland, sparse vegetation; L_n = artificial surfaces, bare area, inland water. See https://stats.oecd.org/Index.aspx?DataSetCode=LAND_COVER#.

and lower share of unusable land are associated with larger welfare gains from recognizing the environmental benefits through the social cost of carbon.

The results reveal that the most welfare gain in terms of percentage increase is in the Sub-Saharan African countries. These countries have low agricultural production and low shares of bare area. They benefit so much mainly because their agricultural production is poor, resulting in low welfare in the benchmark economy. However, recognition of the environmental benefits provided by their land cover produces significant gains in welfare. Meanwhile, countries in Western Europe have the highest welfare in the benchmark economy, with a large comparative advantage in agricultural production. They still have the second-largest welfare among the subregions. However, recognition of environmental benefits has resulted in the transfer of land from agriculture to environmental services and in the smallest percentage increase in welfare. Incorporating the externalities resulted in a convergence of the relative welfare gaps between the subregions.

Absolute welfare is higher in high-income countries when compared with lower-income countries in both the benchmark economy and the experiment. However, lower-income countries benefit more from recognizing the social cost of carbon in the experiment, resulting in a narrower welfare gap between rich and poor countries. Notable are the welfare gains for countries in the Amazon rainforest and Congo Basin regions.[3] The welfare in the experiment is very high for these regions (known as the lungs of the planet) when compared with other subregions. Their initial welfare is fairly high, but they benefit more than most of the subregions of the world in terms of their percentage increase in welfare resulting in extremely high welfare after the experiment.

The different results among countries are driven by two factors: (1) the share of land suitable for GHG sequestration and (2) the comparative advantage between agriculture and sequestration. Three types of land are in the model: (1) land used for production purposes, (2) land used for sequestration purposes, and (3) bare area (such as deserts) that cannot be used for either production or sequestration. Having a higher share of bare area is associated with lower welfare by limiting the land input for both purposes. The countries in Amazon rainforest (3.63 percent) and Congo Basin (1.02 percent) have very low shares of bare area, which enables higher welfare. The relative marginal payoffs between agriculture and sequestration imply that efficiency is maximized by focusing sequestration where agricultural potential is relatively lower and where sequestration opportunities are higher. Therefore, countries that have higher agricultural productivity (mostly high-income countries) will gain less welfare in the process of converting farms to forests.

Table B.8 Experiment results, by country income group

Country income group	Parameters			Aggregate results				
Region	A_a	γ	L_n(%)	W_{BE}	$W_{BE}Rank$	W_{EXT}	$W_{EXT}Rank$	$W(\Delta\,\%)$
Sub-Saharan Africa	23.50	0.41	10.62	0.79	6	3.77	6	380.40
South Asia	32.98	0.39	13.35	0.87	5	3.86	5	346.24
Europe and Central Asia	47.50	0.30	7.31	0.96	3	4.05	2	327.53

[3] Amazon rainforest countries are Bolivia, Brazil, Colombia, Ecuador, Guyana, Peru, República Bolivariana de Venezuela, and Suriname. Countries in the Congo Basin are Cameroon, Central African Republic, Democratic Republic of Congo, Equatorial Guinea, Gabon, and Republic of Congo.

Country income group	Parameters			Aggregate results				
Region	A_a	γ	L_n(%)	W_{BE}	$W_{BE}Rank$	W_{EXT}	$W_{EXT}Rank$	W(Δ %)
Latin America and the Caribbean	41.57	0.34	4.30	0.95	4	4.05	3	326.44
East Asia and Pacific	45.96	0.35	6.18	0.97	2	4.04	4	318.77
North America	60.91	0.28	11.59	1.06	1	4.13	1	290.02
Middle East and North Africa	33.01	0.36	71.80	0.72	7	2.60	7	263.40
Subregion	A_a	γ	L_n(%)	W_{BE}	$W_{BE}Rank$	W_{EXT}	$W_{EXT}Rank$	W(Δ %)
Southern Africa	21.25	0.34	5.74	0.73	18	3.81	14	443.73
Eastern Africa	20.59	0.42	8.99	0.77	17	3.78	15	389.80
Western Africa	24.62	0.42	15.20	0.80	15	3.69	17	364.61
Central Africa	27.63	0.39	7.34	0.84	14	3.87	13	361.88
Eastern Europe	32.04	0.31	4.86	0.88	12	3.99	11	357.09
Caribbean	40.30	0.34	3.39	0.91	11	4.01	10	348.70
Melanesia	38.88	0.36	1.92	0.93	10	4.03	9	339.28
Southern Asia	33.33	0.39	20.07	0.87	13	3.76	16	337.71
Southern Europe	40.32	0.30	3.87	0.95	9	4.06	5	332.30
Central America	41.20	0.36	3.18	0.96	8	4.05	8	322.47
Southeast Asia	42.58	0.37	2.44	0.96	6	4.06	7	322.38
South America	42.23	0.33	5.35	0.96	7	4.06	6	321.67
Eastern Asia	48.77	0.34	16.44	0.97	5	3.95	12	309.34
Northern Europe	63.46	0.28	6.99	1.05	4	4.16	3	299.56
Western Asia	33.65	0.34	52.21	0.78	16	3.03	18	297.88
North America	60.91	0.28	11.59	1.06	3	4.13	4	290.02
Northern Africa	19.66	0.37	72.26	0.61	19	2.42	19	287.50
Australia and New Zealand	68.36	0.28	5.86	1.09	2	4.21	1	285.05
Western Europe	79.46	0.28	11.11	1.13	1	4.20	2	272.76
Income group	A_a	γ	L_n(%)	L_e (%)	L_a (%)	W_{BE}	W_{EXT}	W (Δ %)
High-income	57.61	0.28	12.11	79.98	7.91	1.02	4.01	295.71
Upper-middle-income	36.56	0.33	14.59	76.46	8.95	0.88	3.79	331.66
Lower-middle-income	32.80	0.38	10.15	79.30	10.55	0.88	3.87	345.91
Low-income	21.33	0.43	16.65	72.40	10.95	0.76	3.66	380.10
Lungs of the planet	A_a	γ	L_n(%)	L_e (%)	L_a (%)	W_{BE}	W_{EXT}	W (Δ %)
Amazon rainforest	42.74	0.34	3.63	86.20	10.17	0.97	4.07	321.75
Congo Basin	27.26	0.38	1.02	87.25	11.73	0.85	3.94	368.82

Source: Original table for this publication.

References

Adamopoulos, T., and D. Restuccia. 2014. "The Size Distribution of Farms and International Productivity Differences." *American Economic Review 104* (6): 1667–97.

Adamopoulos, T., and D. Restuccia. 2020. "Land Reform and Productivity: A Quantitative Analysis with Micro Data." *American Economic Journal: Macroeconomics 12* (3): 1–39.

Aguiar, A., M. Chepeliev, E. Corong, R. McDougall, and D. van der Mensbrugghe. 2019. "The GTAP Data Base: Version 10." *Journal of Global Economic Analysis* 4 (1): 1–27. https://www.jgea.org/ojs/index.php/jgea/article/view/77.

Bauer, S. E., K. Tsigaridis, and R. Miller. 2016. "Significant Atmospheric Aerosol Pollution Caused by World Food Cultivation.: *Geophysical Research Letters* 43: 5394–400.

Bayraktarov, E., M. I. Saunders, S. Abdullah, M. MIlls, J. Beher, H. P. Possingham, P. J. Mumby et al. 2016. "The Cost and Feasibility of Marine Coastal Restoration." *Ecological Applications* 26 (4): 1055–74.

Carpenter, S. R., N. F. Caraco, D. L. Correll, R. W. Howarth, A.N. Sharpley, and V. H. Smith. 1998. "Nonpoint Pollution of Surface Waters with Phosphorus and Nitrogen." *Ecological Applications* 8 (3): 559–68. https://doi.org/10.1890/1051-0761(1998)008[0559:NPOSWW]2.0.CO;2.

Castonguay, A. C., S. Polasky, M. Holden, M. Herrero, D. Mason-D'Crox, C. Godde, J. Chang, et al. 2022. Where's the Beef?" University of Queensland, Queensland, Australia.

Chang, J., P. Ciais, M. Herrero, P. Havlik, M. Campioli, X. Zhang, Y. Bai, et al. 2016. "Combining Livestock Production Information in a Process-based Vegetation Model to Reconstruct the History of Grassland Management." *Biogeosciences* 13(12): 3757–76.

Chaplin-Kramer, R., R. P. Sharp, C. Weil, E. M. Bennett, U. Pascual K. K. Arkema, K. A. Brauman, et al. 2019. "Global Modeling of Nature's Contributions to People." *Science* 366 (6462): 255–58. https://doi.org/10.1126/science.aaw3372.

Damania, R., S. Desbureaux, A. S. Rodella, J. Russ, and E. Zaveri. 2019. *Quality Unknown: The Invisible Water Crisis*. Washington, DC: World Bank.

Delgado, O., J. Miller, B. Sharpe, and R. Muncrief. 2016. "Estimating the Fuel Efficiency Technology Potential of Heavy-Duty Trucks in Major Markets Around the World." Working Paper 14. London: Global Fuel Economy Initiative and the International Council on Clean Transportation. https://www.globalfueleconomy.org/media/404893/gfei-wp14.pdf.

Desbureaux, S., F. Mortier, E. Zaveri, M. T. van Vliet, J. Russ, A. S. Rodella, and R. Damania. 2022. "Mapping Global Hotspots and Trends of Water Quality (1992–2010): A Data Driven Approach." *Environmental Research Letters 17* (11): 114048. https://doi.org/10.1088/1748-9326/ac9cf6.

Dinerstein, E., D. Olson, A. Joshi, C. Vynne, N. D. Burgess, E. Wikramanayake, N. Hahn, et al. 2017. "An Ecoregion-based Approach to Protecting Half the Terrestrial Realm. *BioScience* 67 (6): 534–45. https://doi.org/10.1093/biosci/bix014.

Dinerstein, E., C. Vynne, E. Sala, A. R. Joshi, S. Fernando, T. E. Lovejoy, J. Mayorga, et al. 2019. "A Global Deal for Nature: Guiding Principles, Milestones, and Targets." *Science Advances* 5 (4): 1–18. https://doi.org/10.1126/sciadv.aaw2869.

ESA (European Space Agency). 2015. "CCI Land Cover." https://www.esa-landcover-cci.org/.

ESA (European Space Agency). 2019. "ESA Climate Change Initiative " (dashboard). https://www.esa-landcover-cci.org/.

FAO (Food and Agriculture Organization). 2020. "FAOSTAT" (dashboard), accessed March 7, 2020. https://www.fao.org/faostat/en/#data.

FAO (Food and Agriculture Organization). 2021a. "GLEAM—The Global Livestock Environmental Assessment Model: A Global LCA Model of Livestock Supply Chains." https://www.fao.org/climatechange/42050-09ec47f2ffd4be66e383046681c07df00.pdf

FAO (Food and Agriculture Organization). 2021b. "FAOSTAT: Producer Prices" (dashboard), accessed May 27, 2021. https://www.fao.org/faostat/en/#data/PP.

Favero, A., A. Daigneault, and B. Sohngen. 2020. "Forests: Carbon Sequestration, Biomass Energy, or Both? *Science Advances* 6 (13): eaay6792.

Fetzel, T., P. Havlik, M. Herrero, J. O. Kaplan, T. Kastner, S. C. Kroisleitner, S. Rolinski, et al. 2017. "Quantification of Uncertainties in Global Grazing Systems Assessment." *Global Biogeochemical Cycles* 31: 1089–1102. https://doi.org/10.1002/2016GB005601.

Fick, S. E., and R. J. Hijmans. 2017. "WorldClim 2: New 1km Spatial Resolution Climate Surfaces for Global Land Areas." *International Journal of Climatology* 37 (12): 4302–315.

GIZ. 2019. *International Fuel Prices 2018/19*, https://www.transformative-mobility.org/assets/site/GIZ-IFP-International-Fuel-Prices-Report-2019.pdf.

Gollin, D., D. Lagakos, and M. E. Waugh. 2014. "Agricultural Productivity Differences Across Countries." *American Economic Review 104* (5): 165–70. https://doi.org/10.1257/aer.104.5.165

Galloway, J. N., J. D. Aber, JJ. W. Erisman, S. P. Seitzinger, R.W. Haworth, E. B. Cowling, and B. J. Cosby. 2003. "The Nitrogen Cascade." *BioScience* 53 (4): 341–56.

Grantham, H. S., A. Duncan, T. D. Evans, K. R. Jones, H. L. Beyer, R. Schuster, and J. E. M. Watson. 2020. "Anthropogenic modification of forests means only 40% of remaining forests have high ecosystem integrity." *Nature Communications 11* (1): 1–10. https://doi.org/10.1038/s41467-020-19493-3.

Griscom, B. W., J. Adams, P. W. Ellis, R. A. Houghton, RG. Lomax, D. A. Miteva, W. H. Schlesinger, et al. 2017. "Natural Climate Solutions." *Proceedings of the National Academy of Sciences* 114 (44): 11645–650.

Gu, B., Y. Ge, S. X. Chang, W. Luo, and J. Chang. 2013. "Nitrate in Groundwater of China: Sources and Driving Forces." *Global Environmental Change* 23 (5): 1112–21. https://doi.org/10.1016/j.gloenvcha.2013.05.004.

Herrero, M., P. Havlik, H. Valin, A. Notenbaert, M. C. Rufino, P. K. Thornton M. Blummel, et al. 2013. "Biomass Use, Production, Feed Efficiencies, and Greenhouse Gas Emissions from Global Livestock Systems." *Proceedings of the National Academy of Sciences* 110 (52): 20888–893.

Hertel, T. W. 1997. *Global Trade Analysis: Modeling and Applications.* Cambridge, UK: Cambridge University Press.

Hill, J., A. Goodkind, C. Tessum, S. Thakrar, D. Tilman, S. Polasky, T. Smith, et al. 2019. "Air-Quality Related Health Damages of Maize." *Nature Sustainability* 2 (5): 397–403.

Hudson, L. N., T. Newbold, S. Contu, S. L. Hill, I. Lysenko, A. De Palma, H. R. Phillips, e al. 2014. "The PREDICTS Database: A Global Database of How Local Terrestrial Biodiversity Responds to Human Impacts." *Ecology and Evolution* 4 (24): 4701–735. https://doi.org/10.1002/ece3.1303.

ILO (International Labor Organization). 2021). "ILOSTAT: Statutory Nominal Gross Monthly Minimum Wage." https://www.ilo.org/ilostat-files/Documents/Excel/MBI_542_EN.xlsx.

IPCC (Intergovernmental Panel on Climate Change). 2021. *Climate Change 2021: The Physical Science Basis*. *Contribution of Working Group I to the Sixth Assessment Report of the Intergovernmental Panel on Climate Change*, edited by V. Masson-Delmotte, P. Zhai, A. Pirani, S. L. Connors, C. Péan, S. Berger, N. Caud, et al. Cambridge, UK: Cambridge University Press.

IUCN (International Union for Conservation of Nature). 2016. "A Global Standard for the Identification of Key Biodiversity Areas: Version 1.0." IUCN, Gland, Switzerland.

IUCN (International Union for Conservation of Nature). 2019. "IUCN Red List of Threatened Species." https://www.iucnredlist.org/en.

Johnson, A. J., G. Ruta, U. Baldos, R. Cervigni, S. Chonabayashi, E. Corong, O. Gavryliuk, et al. 2021. *The Economic Case for Nature*. Washington, DC: World Bank.

Kareiva, P., Tallis**,** H., Ricketts, T.H., Daily, G.C., & Polasky, S. (eds.) 2011. *Natural Capital: Theory and Practice of Mapping Ecosystem Services*. Oxford University Press.

Keeler, B., S. Polasky, K. A. BraumanK. A. Johnson, J. C. Finlay, A. O'Neill, K. Kovacs, et al. 2012. "Linking Water Quality and Well-being for Improved Assessment and Valuation of Ecosystem Services." *Proceedings of the National Academy of Sciences* 109: 18619–24.

Kim, J. B., E. Monier, B. Sohngen, G. S. Pitts, R. Drapek, J. McFarland, S. Ohrel, and J. Cole. 2017. Assessing Climate Change Impacts, Benefits of Mitigation, and Uncertainties on Major Global Forest Regions under Multiple Socioeconomic and Emissions Scenarios." *Environmental Research Letters* 12 (4): 045001.

Lal, R. 2002. "Soil Carbon Dynamics in Cropland and Rangeland." *Environmental Pollution* 16 (3): 353–62.

Model, E. A. (2017). The global livestock environmental assessment model. *Food and Agriculture Organization of the United Nations (FAO)*, 22-6. https://www.fao.org/gleam/en/.

Monfreda, C., N. Ramankutty, and J. A. Foley. 2008. "Farming the Planet: 2. Geographic Distribution of Crop Areas, Yields, Physiological Types, and Net Primary Production in the Year 2000." *Global Biogeochemical Cycles* 22: GB1022. https://doi.org/10.1029/2007GB002947.

Mueller, N. D., J. S. Gerber, M. Johnston, D. K. Ray, N. Ramankutty, and J. A. Foley. 2012. "Closing Yield Gaps through Nutrient and Water Management." *Nature* 490 (7419): 254–57. https://doi.org/10.1038/nature11420.

NASA STRM (National Aeronautics and Space Administration Shuttle Radar Topography Mission). (013. "Shuttle Radar Topography Mission (SRTM) Global" accessed March 31, 2022. Distributed by OpenTopography. https://doi.org/10.5069/G9445JDF.

Nelson, E., G. Mendoza, J. Regetz, S. Polasky, H. Tallis, D. R. Cameron, K. M. A. Chan, et al. 2009. "Modeling Multiple Ecosystem Services, Biodiversity Conservation, Commodity Production, and Tradeoffs at Landscape Scales." *Frontiers in Ecology and the Environment* 7 (1): 4–11.

Newbold, T., L. N. Hudson, S. L. L. Hill, S. Contu, I. Lysenko, R. A. Senior, L. Börger, et al. 2015. "Global Effects of land Use on Local Terrestrial Biodiversity." *Nature* 520: 45–50. https://doi.org/10.1038/nature14324.

Olson, D. M., E. Dinerstein, E. D. Wikramanayake, N. D. Burgess, G. V. N. Powell, E. C. Underwood, J. A. D'amico, et al. 2001. "Terrestrial Ecoregions of the World: A New Map of Life on Earth: A New Global Map of Terrestrial Ecoregions Provides an Innovative Tool for Conserving Biodiversity." *BioScience* 51 (11): 933–38. https://doi.org/10.1641/0006-3568(2001)051[0933:TEOTWA]2.0.CO;2.

Olson, D. M., and E. Dinerstein. 2002. "The Global 200: Priority Ecoregions for Global Conservation." *Annals of the Missouri Botanical Garden* 89 (2): 199–224. https://doi.org/10.2307/3298564.

Ouedraogo, I., P. Defourny, and M. Vanclooster. 2019. "Application of Random Forest Regression and Comparison of Its Performance to Multiple Linear Regression in Modeling Groundwater Nitrate Concentration at the African Continent Scale." *Hydrogeology Journal* 27 (3): 1081–98. https://doi.org/10.1007/s10040-018-1900-5.

Ouyang, Z., H. Zheng, Y. Xiao, S. Polasky, J. Liu, W. Xu, Q. Wang, et al. 2016. "Improvements in Ecosystem Services from Investments in Natural Capital." *Science* 352: 1455–59.

Polasky, S., E. Nelson, J. Camm, B. Csuti, P. Fackler, E. Lonsdorf, C. Montgomery, et al. 2008. "Where to Put Things? Spatial Land Management to Sustain Biodiversity and Economic Returns." *Biological Conservation* 141 (6):1505–24.

Ray, D. K., P. C. West, M. Clark, J. S. Gerber, JA. V. Prishchepov, and S. Chatterjee. 2019. "Climate Change Has Likely Already Affected Global Food Production." *PLoS ONE* 14 (5): e0217148. https://doi.org/10.1371/journal.pone.0217148.

Restuccia, D., and R. Santaeulalia-Llopis. 2015. "Land Misallocation and Productivity." Working Paper 541. University of Toronto, Department of Economics. https://www.economics.utoronto.ca/public/workingPapers/tecipa-541.pdf.

Restuccia, D., D. T. Yang, and X. Zhu. 2008. "Agriculture and Aggregate Productivity: A Quantitative Cross-Country Analysis." *Journal of Monetary Economics 55* (2): 234–50. https://doi.org/10.1016/j.jmoneco.2007.11.006.

Rosa, L., D. D. Chiarelli, C. Tu, M. C. Rulli, and P. D'Odorico. 2019. "Global Unsustainable Virtual Water Flows in Agricultural Trade." *Environmental Research Letters* 14: 114001. https://doi.org/10.1088/1748-9326/ab4bfc.

Ruesch, A., and H. K. Gibbs. 2008. "New IPCC Tier-1 Global Biomass Carbon Map for the Year 2000." Carbon Dioxide Information Analysis Center, Oak Ridge National Laboratory, Oak Ridge, TN. http://cdiac.ess-dive.lbl.gov.

Santaeulalia-Llopis, R., and D. Restuccia, D. 2014. "Land Misallocation and Productivity." In *2014 Meeting Papers* (No. 1314). Society for Economic Dynamics.

Sharp, R., J. Douglass, S. Wolny, K. Arkema, J. Bernhardt, W. Bierbower, N. Chaumont, et al. 2020. "InVEST 3.10.2.post24+ug.g99a876b.d20220317 User's Guide." Natural Capital Project, Stanford University, University of Minnesota, Nature Conservancy, and World Wildlife Fund.

Siikamäki, J., and F. Santiago-Ávila. 2014. "Improving the Forest Database to Support Sustainable Forest Management." Working paper, Resources for the Future, Washington, DC.

Smith, J. R., A. D. Letten, P.-J. Ke, C. B. Anderson, J. H. Hendersot, M. K. Dhami, G. A. Dlott, et al. 2018. "A Global Test of Ecoregions." *Nature Ecology and Evolution* 2: 1889–96. https://doi.org/10.1038/s41559-018-0709-x.

Suh, S., J. A. Johnson, L. TambjergS. Sim, S. Broeckx-Smith, W. Reyes, and R. Chaplin-Kramer. 2020. "Closing Yield Gap Is Crucial to Avoid Potential Surge in Global Carbon Emissions." *Global Environmental Change* 63: 102100. https://www.sciencedirect.com/science/article/pii/S0959378019311021.

Temkin, A., S. Evans, T. Manidis, C. Campbell, and O. V. Naidenko. 2019. "Exposure-based Assessment and Economic Valuation of Adverse Birth Outcomes and Cancer Risk Due to Nitrate in United States Drinking Water." *Environmental Research* 176: 108442.

TEEB (The Economics of Ecosystems and Biodiversity). 2009. "Climate Issues Update." http://www.teebweb.org/media/2009/09/TEEB-Climate-Issues-Update.pdf.

Tian, X., B. Sohngen, J. B. Kim, S. Ohrel, and J, Cole. 2016. "Global Climate Change Impacts on Forests and Markets." *Environmental Research Letters* 11 (3): 035011.

Valentinyi, A., and B. Herrendorf. 2008. "Measuring Factor Income Shares at the Sectoral Level." *Review of Economic Dynamics 11* (4): 820–35. https://doi.org/10.1016/j.red.2008.02.003.

Waldron, C. D., L. Q. Maurice, M. Kapshe, D. M. Allyn, M. Locke, S. Lukachko, and S. Pesmajoglou. 2006. "Mobile Combustion." In *2006 IPCC Guidelines for National Greenhouse Gas Inventories* (Vol. 2), edited by S. Eggelston, L. Buendia, K. Miwa, T. Ngara, and K. Tanabe Intergovernmental Panel on Climate Change, 3.1–3.78. Institute for Global Environmental Strategies. https://www.ipcc-nggip.iges.or.jp/public/2006gl/pdf/2_Volume2/V2_3_Ch3_Mobile_Combustion.pdf.

Weiss, D. J., A. Nelson, H. S. Gibson, W. Temperley, S. Peedell, A. Lieber, M. Hancher, et al. 2018. "A Global Map of Travel Time to Cities to Assess Inequalities in Accessibility in 2015. *Nature* 553 (7688): 333–36.

World Bank. 2020. *The Changing Wealth of Nations 2021: Managing Assets for the Future*. Washington, DC: World Bank. doi: 10.1596/978-1-4648-1590-4.

Zabel, F., B. Putzenlechnerand W. Mauser. 2014. Global Agricultural Land Resources: A High Resolution Suitability Evaluation and Its Perspectives until 2100 under Climate Change Conditions. *PLoS ONE* 9(9): e107522.